The Interpretation of Charged Particle Measurements on Laser Produced Plasmas

B. W. Nicholson

Report No. 96
March, 1980

CHAPTER I

INTRODUCTION

When a target is irradiated by a high power laser a hot ionized plasma is produced. Hydrodynamic forces cause this plasma to rapidly expand outward into the surrounding vacuum. As a consequence of this expansion, the thermal energy created by the absorption of the laser light becomes kinetic energy of the ions streaming away from the target's original location. These ions can be detected as ion current and used as a diagnostic of the interaction between the incident laser energy and the target material. This thesis investigates that relationship.

Historically the dominant feature of the ion flux of a laser produced plasma has been the presence of two distinct velocity components.[1,2,3,4] For small laser energies the slower of these two components rapidly recombines and is not detected as part of the ion current. However for larger laser energies both components remain charged and appear as peaks in the measured current as is seen in Figure 1. For incident laser energies of 5 - 15 joules in a short pulse of nominally 50 psec, the slower peak in the ion current has a velocity on the order of $1 - 2 \times 10^7$ cm/sec. It will be referred to as the slow ion peak. It is preceeded by a

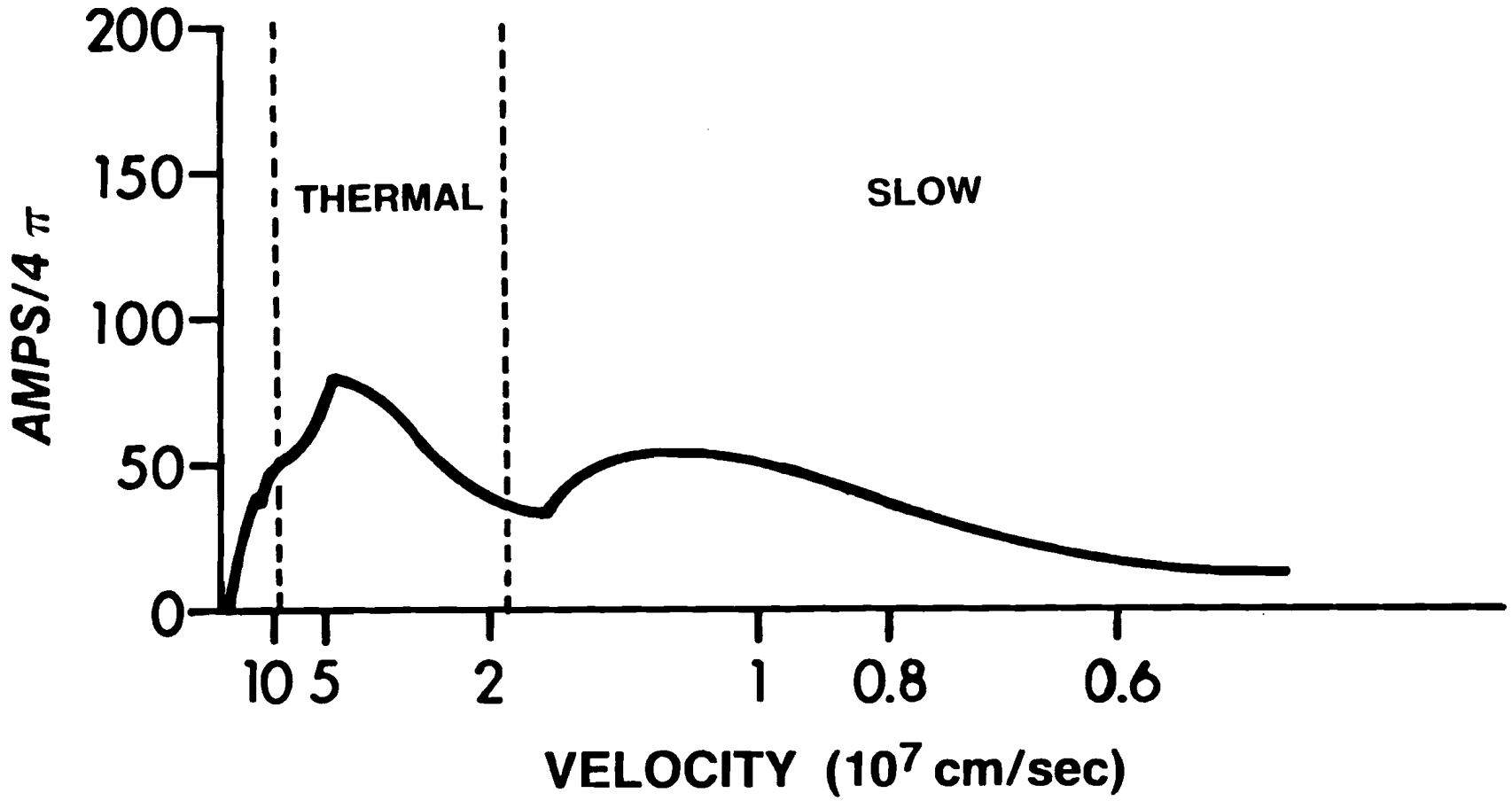

Figure 1.

Charge Collector Current for Shot 17549.

8.6 joules (76 psec FWHM) incident on a glass microballoon. The target diameter was 70 microns; the wall thickness was 0.76 microns.

peak with a velocity of 3 - 5 x 10^7 cm/sec which will be called the thermal peak. Additionally there is sometimes a third, somewhat smaller peak of fast ions with velocities greater than 10^8 cm/sec. This is evident in the figure only as a shoulder on the leading edge of the thermal peak. These fast ions make up only about 1% of the target mass[5] and have been shown to be a surface phenomenon, therefore they will be ignored in the following discussion.

Previous work at the University of Rochester using hollow spherical glass targets (microballoons) has tenatively identified fied the thermal peak ions as that portion of the target which is ablated away by the incident laser energy. X-ray measurements[6] indicate the absorption region attains a 1 kev temperature which highly ionizes the silicon and oxygen of the glass shell. The corresponding expansion velocity, v, can be estimated as

$$v \simeq \sqrt{\frac{3(Z + 1)\, T}{A}} \times 10^6 \text{ cm/sec} \qquad (1)$$

where the plasma temperature, T, is in electron volts and the average ion has mass number A and charge Z. For a fully ionized glass target A = 20 and Z = 10 so that the expected expansion velocity is 4 x 10^7 cm/sec. This is in agreement with the observed velocity of the thermal peak of the ion current.

The remainder of the target material never directly sees the laser and therefore is expected to be cooler. X-ray line measurements[6] from neon-filled targets indicate that a temperature of a few

hundred electron volts is appropriate for the interior of the target. This material will expand with the observed velocity of the slow ion peak.

This simple example which relates the gross structure of the ion current to the distribution of energy within the target at early times indicates the potential value of charge particle measurements as a method of investigating the mechanism of energy deposition and transport within the target. In the past this sort of analysis has been impeded by the fact that the ion current is not a single quantity but is a combination of two variables, the ion flux and the asymptotic ion charge state. Hence in principle shot to shot variations in the observed ion current are ambiguous in the sense that they could be due to independent changes in either of the two underlying variables; and, while it is straightforward to measure the current, it is much more tedious to measure either the ion charge states or the ion flux. Hence the interpretation of the ion current is not one problem but two.

In the following, both measurements and numerical simulations will be presented which show that the two problems are in fact independent, and that the asymptotic charge state of the ions as a function of velocity is insensitive to the interactions which determine the ion flux. Hence in practice changes in the ion

current contain no ambiguity. They always reflect changes in the velocity spectrum of the ion expansion due to variations in the energy deposition of the laser-target interaction.

The asymptotic charge state of the plasma is determined by the electron - ion recombination which occurs after the expansion has reached its asymptotic velocity. The time scale of interest is the tens of nanoseconds it takes the plasma to disperse. The dominant physics is the balance between radiative and collisional processes in dissipating the binding energy released by recombination.

The ion flux on the other hand is determined by the target dynamics which occur before the expansion becomes asymptotic. For the small isolated targets used here this is in the first few tenths of a nanosecond. The flux is determined by the energy absorption and transport within the target during this time. For example, if more energy is deposited in the target a hotter plasma is produced. The corresponding increase in the plasma pressure leads to a faster expansion of the target material. Thus a larger ion current will be detected due to the increased ion flux. The ion flux is not affected by the subsequent changes in the charge state due to recombination because by then the kinetic energy of the streaming ions is much greater than the ionizational potential energy available to the plasma through recombination.

The distinct time scales which separate the physics of the target dynamics from the recombination which determines the plasma charge state is most obvious in the slower of the two velocity components of the asymptotic ion current. It is for these velocities that recombination significantly alters the initial ion charge states. Therefore, the following analysis will emphasize this slow component of the plasma where the bulk of the target material is to be found.

Chapter II examines the atomic processes which determine the final ionization state of the plasma. Asymptotically collisional (3-body) recombination becomes the most important process occurring in the plasma. If the plasma can disperse quickly enough it will remain charged. If it cannot disperse quickly, 3-body recombination will have sufficient time to completely neutralize the plasma ions. Simple analytic expressions show that the collisional thermalization of the ion's binding energy as a part of 3-body recombination is essential to maintaining a charged plasma during the expansion.

Measurements of both the asymptotic ion charge states and the total ion current are presented in Chapter III. These results show that the final charge state of the ion as a function of velocity is not affected by changes in the incident laser energy. However, energy variations do produce a response in both the amplitude and velocity of the two peaks in the ion current.

The same behavior is found in the numerical simulation described in Chapter IV. In addition the simulation indicates that different models of the energy deposition and transport within target change features of the ion current without changing the final charge state of the plasma. Details of the rate equation calculation of the ion charge state are found in Appendix A.

The operational requirements and principles of the prime diagnostic of this experiment, an electrostatic analyzer (mass spectrometer), are found in Appendix B.

REFERENCES - CHAPTER I

1. Seka, W., Scwob, J. L., and Breton, C. J. Appl. Phys. 41 3440 (1970).
2. Rumsby, P. T. and Paul, J. W. M. Plasma Physics 16 247 (1974).
3. Pelah, I., Goldman, E. B., and Yaakobi, B. Phys. Rev. Lett. 37 829 (1976).
4. Goforth, R. R. and Hammerling, P. J. Appl. Phys. 47 3918 (1976).
5. Slater, D. C., Mayer, F. J., and Pearlman, J. S., KMSF-U674 (November 1977).
6. Thorsos, E. I., Delettrez, J. A. and Goldman, E. B. Laboratory for Laser Energetics Report #59 (August 1977).

CHAPTER II

THE CHARGE STATE OF AN EXPANDING PLASMA

The charge state of a plasma is a time dependent competition between the rates of the ionization and recombination processes. When a plasma is created by the absorption of laser light, it initially has a high density and a temperature of several hundred electron volts. Under these conditions collision rates are sufficient to establish and maintain an ionizational equilibrium. Thus the charge state of the plasma rapidly approaches complete ionization. Later, after the laser pulse, hydrodynamic and radiative processes cool and disperse the plasma causing the equilibrium charge state to fall with the falling temperature. However, as will be discussed below, the rapid dispersion of the plasma through hydrodynamic expansion produces conditions in which the collision rate will be inadequate to maintain ionizational equilibrium. This provides an interval where the measured charge state is temporarily much larger than the equilibrium value for that temperature and density.

In order to model this process it is necessary to follow the time history of individual plasma elements using a set of ionizational rate equations. The charge state of each region of these plasma is found by integrating these rate equations from a time of ionizational equilibrium to the time of interest. Typically such rate equations (one for each ionic species present) are written:

$$\frac{dn_i^Z}{dt} = (S_i^Z - \alpha_i^Z)\, n_e\, n_i^Z \qquad (2)$$

where n_e is the electron density and n_i^Z is the ion density for ions of type i with charge Z. S and α are coefficients describing the net rates of the ionization processes and the recombination processes. (Although this notation is explicitly a two body formulation, additional density dependences may be implicit in the coefficients.)

A time dependent solution to these rate equations requires a detailed numerical simulation. This has been done and in Chapter IV the results of the model will be examined in relation to the measured behavior of the plasma. Some of the details of this model can be found in Appendix A. However here, a review of the relevant atomic processes can identify the important variables and provide a basis for understanding the qualitative behavior of the plasma charge state. Figure 2 illustrates the ionization and recombination mechanisms which will be considered. In general the coefficients corresponding to these processes can be expressed by analytic formulas that are thought to be accurate to about a factor of three.[1] (An exception to this is the 3-body collisional recombination coefficient where the experimental value of the rate coefficient has recently been revised downward by almost an order of magnitude.)[2]

Ionization

In the absence of incident laser radiation the temperatures and densities involved make electron impact the only ionization

process. As shown schematically in Figure 2, this process involves a free electron striking an atom with sufficient energy to cause ionization. The collisionally ionized electron need not be from the atom's outer shell, but the strong temperature dependence of the ionization cross section makes it unnecessary to consider states more tightly bound than the next shell in. The ionization coefficient is given by[1]

$$S = \frac{2.5 \times 10^{-6}}{I^{3/2}} \quad \frac{n\,(T/I)^{1/2}}{1 + (T/I)}\; e^{-I/T}\ \mathrm{cm}^3\ \mathrm{sec}^{-1} \qquad (3)$$

where the ionization potential, I, and the temperature, T, are in electron volts. n is the number of equivalent electrons in the shell considered.

Recombination

In contrast to this single ionization process Figure 2 illustrates several possible recombination mechanisms (dielectronic, radiative, and 3-body collisional processes). These will be treated as independent processes whose sum gives the total recombination coefficient. Bates *et al.*[3] have shown that there are some plasma conditions in which this assumed independence is not correct. However, the recombination rate with the appropriate corrections does not differ greatly. Furthermore a rapidly expanding plasma quickly passes through the regions where plasma conditions allow more than one important mechanism for recombination. The plasma spends most of its time in regimes where the independence of the processes is a

ATOMIC PROCESSES

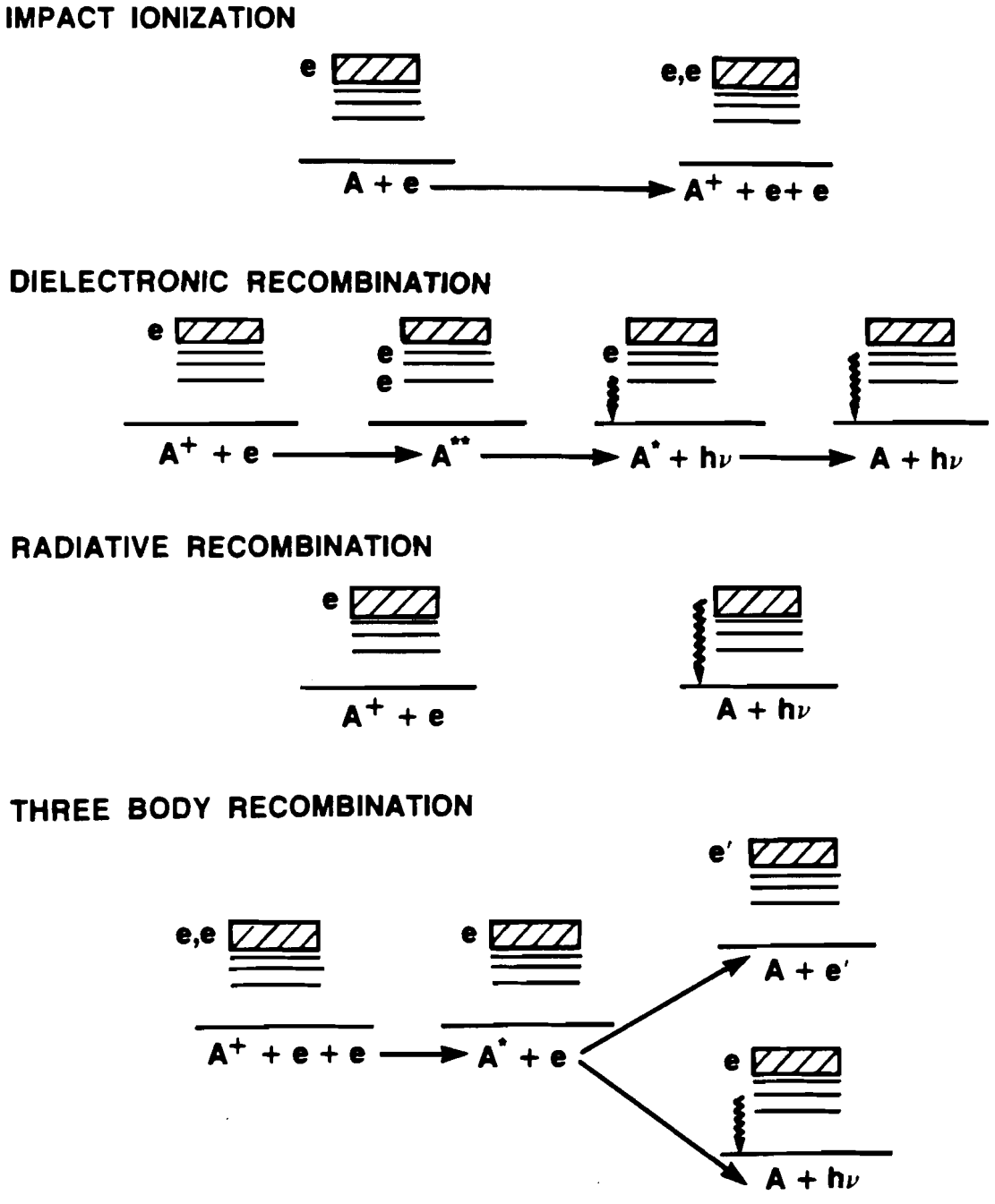

Figure 2. Atomic Processes in an Expanding Laser Processed Plasma

(see text for discussion)

good assumption because a single dominant recombination process determines the total recombination rate.

Dielectronic recombination describes the process in which an ion is struck by a free electron with just the right energy to resonantly excite one of the bound electrons. This results in the capture of the incident electron and creates a doubly excited atom. (A** in the figure) Radiative de-excitation may ensue if the collision rate is sufficiently low so that the upper excited state is not reionized.[4] Thus for dielectronic recombination to be important the plasma must simultaneously have a temperature[4,5] on the order of the atom's ionization energy and a density[6,7] below about 10^{16} cm^{-3}.

These conditions may be present in a steady state plasma such as the solar corona where dielectronic recombination is important in determing the equilibrium charge state. However, an inertial confinement plasma is formed at high densities where collisional processes prevent radiative stabilization of the excited atom. Dielectronic recombination has a temperature dependence[5,8] of $T^{-3/2}\ e^{-\Delta E/kT}$, where ΔE is the excitation energy of the resonant state. Subsequently, when the density drops due to expansion, the plasma is cooled and quickly becomes too cold for dielectronic recombination. Therefore although it was included in the computer simulation, dielectronic recombination is not important in determining

the asymptotic charge state of an expanding plasma.

Direct capture of an electron through a radiative transition from the continuum is of more interest since its probability increases with falling temperature. Seaton[2,9] has calculated the radiative recombination coefficient to be

$$\alpha_R = 5.2 \times 10^{-14} Z (I/kT)^{1/2} (0.429 + .5 \times \ln(I/kT) + 0.469 (I/kT)^{-1/3}) \ cm^3 \ sec^{-1} \quad (4)$$

and this form was used in the numerical model. However, for the purposes of this discussion the above may be approximated as a simple power law[10] fit

$$\alpha_R = 2.7 \times 10^{-13} Z^2 T^{-3/4} \ cm^3 \ sec^{-1} \quad (5)$$

where T is in electron volts. (These two expressions are in order of magnitude agreement for $.1 \text{ ev} \leq T \leq 50$ ev.)

The other process which increases with falling temperature is 3-body combination. This involves a collision between two free electrons in the Coulomb field of an ion, and results in one of the electrons being captured in a state with binding energy $\simeq kT_e$. Since bound states near this level are separated by energies of much less than kT_e, further collisions can rapidly deexcite the captured electron until the energy levels become separated by kT_e. Further deexcitation can occur either by collisional or radiative

processes depending on the density of the plasma. In the Hinnov-Hirschberg model[11] the rate determining step for the recombination is the original collisional capture of the electron.

The rate coefficient for this process is given by[12]

$$a_3 = 0.88 \times 10^{-26} Z^3 T^{-9/2} \ln(\sqrt{Z^2 + 1}) n_e \qquad (6)$$

$$\simeq 0.5 \times 10^{-26} Z^3 T^{-9/2} n_e$$

where the proportionality constant has been experimentally determined but should be substantially lower according to the revised measurements of Hinnov and Johnson. However, the deexcitation pathway is important in the energy balance of the plasma. Ionizational potential energy is either collisionally converted to thermal energy of the free electrons or it is radiated away.

Asymptotic Behavior of the Plasma

The relative importance of the recombination processes in determining the final charge state of the plasma can be illustrated by temporarily ignoring any heat gained from 3-body recombination. Consider the adiabatic expansion of a fluid. After a few radii of expansion the thermal energy of each fluid element becomes negligible compared to its kinetic energy. The expansion velocity then approximates its asymptotic value and the temperature and density scaling is given by

$$n_i,\ n_e \sim r^{-3} \sim t^{-3}$$
$$T \sim r^{-2} \sim t^{-2} \tag{7}$$

Using this scaling in the recombination coefficients it is noted that dielectronic recombination becomes exponentially small and that the relative importance of radiative capture to 3-body recombination diminishes as $t^{-4.5}$. When expansion cooling causes the temperature to fall below the point where

$$n_e > \frac{3 \times 10^{13}\ T_e^{3.75}}{Z}\ cm^{-3} \tag{8}$$

3-body collisions become the dominant recombination process. Thereafter it is the only recombination process of interest.

Impact ionization is a competing process while the electron temperature remains high. But its exponential temperature dependence makes it unimportant as soon as the plasma temperature drops below the atom's ionization energy. Asymptotically the dominant process in opposition to recombination is the spherical expansion of the plasma. By rapidly lowering the electron density, expansion inhibits the collisions which lead to recombination. But for an adiabatic expansion dispersing the plasma is not sufficient to maintain a charge. This is seen by comparing the rate of decline in the electron density due to expansion to that due to 3-body recombination. The expansion becomes progressively less important since adiabatic scaling changes the density at a rate

$$\left(\frac{dn}{dt}\right)_E \sim t^{-4} \tag{9}$$

while the rate of recombination remains constant

$$\left(\frac{dn}{dt}\right)_3 \sim n_e^2 \; n_i \; T^{-9/2} \sim t^0. \tag{10}$$

Asymptotically the plasma would become neutral.

However let us return to the consequences of transferring energy to the free electrons during the collisional deexcitation of the ions as occurs in 3-body recombination. As noted by Kuznetsov and Raizer[13] in 1965 this causes a slower cooling of the plasma than would occur in an adiabatic expansion. It is easy to estimate how much modification of the plasma's temperature scaling is required to produce a non-zero asymptotic charge. Equations 2) and 6) give the rate of electron loss through 3-body recombination as

$$\left(\frac{dn_e}{dt}\right)_3 = \sum_Z \alpha_3 n_e n_i^Z$$

This expression may be simplified by assuming that all of the ions are in the average charge state <Z> given by

$$\langle Z \rangle = \frac{n_e}{n_i}$$

where the total ion density

$$n_i = \sum_Z n_i^Z$$

is not changed by 3-body recombination.

Thus

$$n_i \frac{d\langle Z\rangle}{dt} \simeq -0.5 \times 10^{-26} \langle Z\rangle^5 \, n_i^3 \, T^{-9/2} \tag{11}$$

or

$$d\langle Z\rangle \langle Z\rangle^5 \sim n_i^2 \, T^{-9/2} \, dt$$

And since n_i still scales hydrodynamically as $n_i \sim t^{-3}$, $\langle Z\rangle$ has non-zero asymptotic values if $T \sim t^{-m}$ with $m < 10/9 \simeq 1$. This revised temperature scaling can not occur until 3-body collisions become a significant source of recombination. Nor does it prevent the asymptotic dominance of the 3-body process over the other recombination mechanisms (see Figure 3). But as long as enough heat is provided to maintain the required temperature scaling, recombination is unable to neutralize the plasma before it disperses. Thus the important parameter in the expansion is the amount of the ionization potential which is converted into electron thermal energy during the recombination process. If this energy produces little heating the plasma expansion remains close to adiabatic ($m = 2$) and complete neutralization occurs. However, if the heating is significant ($m \simeq 1$) 3-body recombination becomes a self-limiting

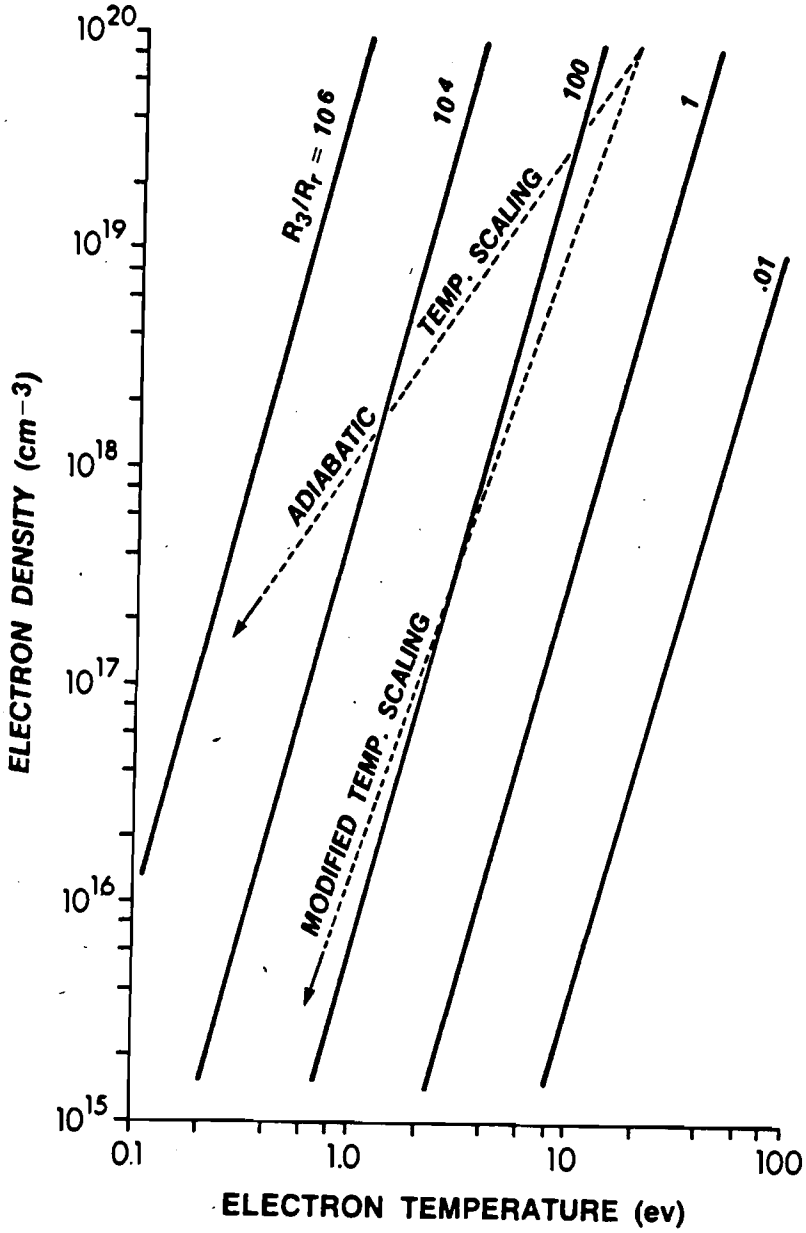

Figure 3.
The Asymptotic Dominance of 3-Body Recombination.

The ratio of collisional recombination, R_3, to radiative recombination, R_r, increases with time for plasma expansions which have either adiabatic or the modified temperature scaling due to 3 body recombination.

process which freezes the charge state at non-zero value.

An estimate of the amount of thermal energy made available by 3-body recombination was included in the work of Kuznetsov and Raizer. The ion is assumed to be hydrogenic with a charge Z and to have captured a single electron which starts in a high quantum number state. The initial deexcitation of this electron is collisional. But, since collisional transitions become slower at lower quantum numbers while radiative transitions become faster, there is a level for which the two deexcitation mechanisms become equally probable. This level, where the rate of collisional decay equals the rate of radiative decay, is called the collisional limit. It is assumed that all the binding energy below the collision limit is lost through radiation while that above the collision limit is thermalized via collisions.

By calculating the collision limit one finds the net energy, E^*, which is given to the plasma electrons by each recombination. For a plasma of density N_e (cm^{-3}) and temperature T (ev), E^* is given by

$$E^* = \min \left\{ \begin{array}{l} 5.4 \times 10^{-5} \; Z^{2/3} \; N_e^{1/3} \; T^{-1/2} \\ 9.2 \times 10^{-3} \; Z^{2/3} \; N_e^{1/6} \; T^{1/12} \\ \text{Ionization Potential} \end{array} \right\} \text{ ev} \qquad (12)$$

This value of E^* is in agreement with the numerical calculations of Bates and Kingston[13] for optically thin hydrogen plasmas. However, optically thick plasmas retain a much larger portion of the ionization energy than is indicated by this formulation.

REFERENCES - CHAPTER II

1. Griem, H. R. and Loveberg, R. H. (volume eds.) Methods of Experimental Physics, Vol. 9A, Chapter 4, Marton, L. (ed. in chief) Academic Press, New York (1970).
2. Johnson, L. C. and Hinnov, E. J. Quant. Spectrosc. Radiat. Transfer. 13, 333 (1973).
3. Bates, D. R., Kingston, A. E. and McWhirter, R. W. P. Proc. Roy. Soc. A267 297 (1962).
4. Donalson, T. P. CLM-R153 (March 1976).
5. Shore, B. W. Astrophys. J. 158 1205 (1969).
6. Davis, J., Jacobs, V. L., Kepple, P. C. and Blaha, M. J. Quant. Spectrosc. Radiat. Transfer 17 139 (1977).
7. Weisheit, J. C. J. Phys. B. 8 2556 (1975).
8. Burke, P. G. and
and Applications, Chapter 6, North Holland, Amsterdam (1976).
9. Seaton, M. J. M. N. 119 81 (1959).
10. Allen, C. W. Astrophysical Quantities, Athlone Press, London.
11. Hinnov, E. and Hirschberg J. G. Phy. Rev. 125 795 (1962).
12. Gurevich, A. V. and Pitaevskii, L. P. JEPT 19 870 (1964).
13. Kuznetsov, N. M. and Raizer, Yu. P. Journal Appl. Mech. Tech. Phys. 4 6 (1965).
14. Bates, D. R. and Kingston, A. E. Proc. Roy. Soc. Lond. 279A 10 (1964).

CHAPTER III

EXPERIMENTAL RESULTS

The objective of this experiment was to obtain a quantitative measurement of the charge state distribution present at plasma velocities between 0.5 and 2 x 10^7 cm/sec. The total ion current shows a broad peak in this velocity region when mass limited targets are hit by 5 - 10 joules of laser energy in a short (50 - 100 psec) pulse. The precise form of the target does not appear to matter since qualitatively similar ion currents are observed for solid glass spheres[1] or cylinders as well as the usual hollow glass microballoon targets. It has been proposed that this structure in the ion current contains the material from the inside of the target and thus may provide information about the energy transported to the target interior.[2]

The primary diagnostic of the experiment was a mass spectrometer which measured the ion current for each ion charge to mass ratio, A/Z, present in the plasma. The operation of this variety of mass spectrometer, also referred to as an electrostatic analyzer, is illustrated in Figure 4. A drift length, L, in this case 154 cm, separates plasma velocities by time of flight. Then the electrostatic field of a parallel plate capacitor separates the ions by their energy per unit charge. Each detector within the mass

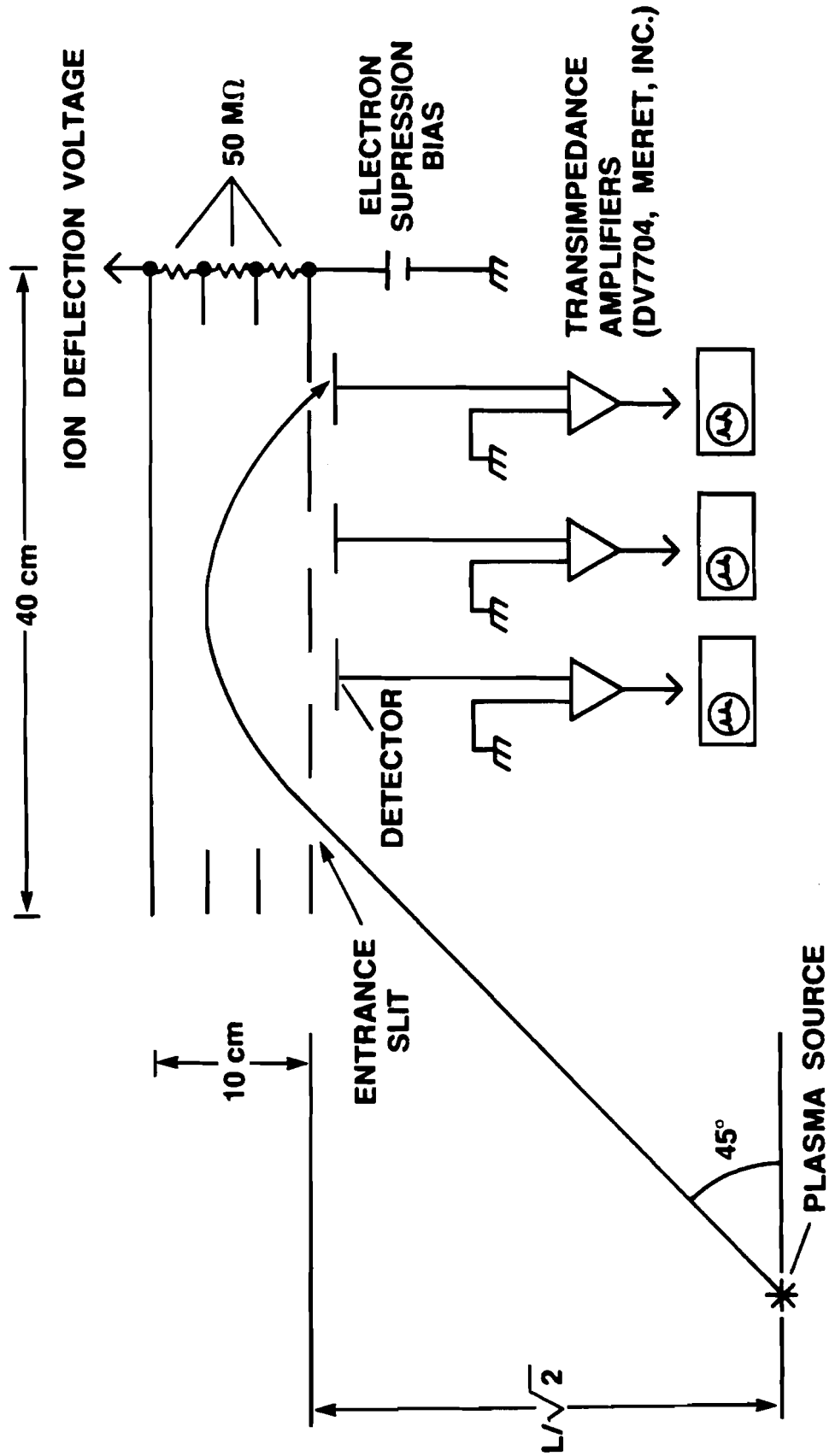

Figure 4. Schematic of Mass Spectrometer Operation.

spectrometer receives a particular energy per unit charge and distinguishes different charge to mass ratios on the basis of arrival time. (A more complete description of the operation of this instrument may be found in Appendix B.) In order to prevent the occurrence of charge exchange as the ions travelled from the target site to the detectors in the mass spectrometer both the target chamber and spectrometer were kept at a pressure of less than 10^{-6} mm of Hg.

The plasmas analyzed in this experiment were produced by the Delta laser system of the Laboratory for Laser Energetics. This four beam Neodynium glass system (λ = 1.06μ) was used to provide symmetric illumination of the spherical targets in the plane perpendicular to the slender stalk from which each target is mounted (see Figure 5). The nominal laser pulse had a FWHM of 50 psec and provided an energy on target of 5 - 6 joules. Calorimeters measured the energy in each shot and the time history of the laser power was recorded on an optical streak camera. Focusing of each beam to a 30μ spot on the target surface provided an incident intensity of a few times 10^{15} watts/cm^2.

Other experiments which were performed concurrently provided auxiliary plasma diagnostics. A full description of these concurrent experiments may be found in References 4 and 5. Only those diagnostics of direct interest to the interpretation of charged particle measurements will be mentioned here. Chief among these was a set of charge collectors, Faraday cups biased to reject plasma electrons. These were located at various positions around the

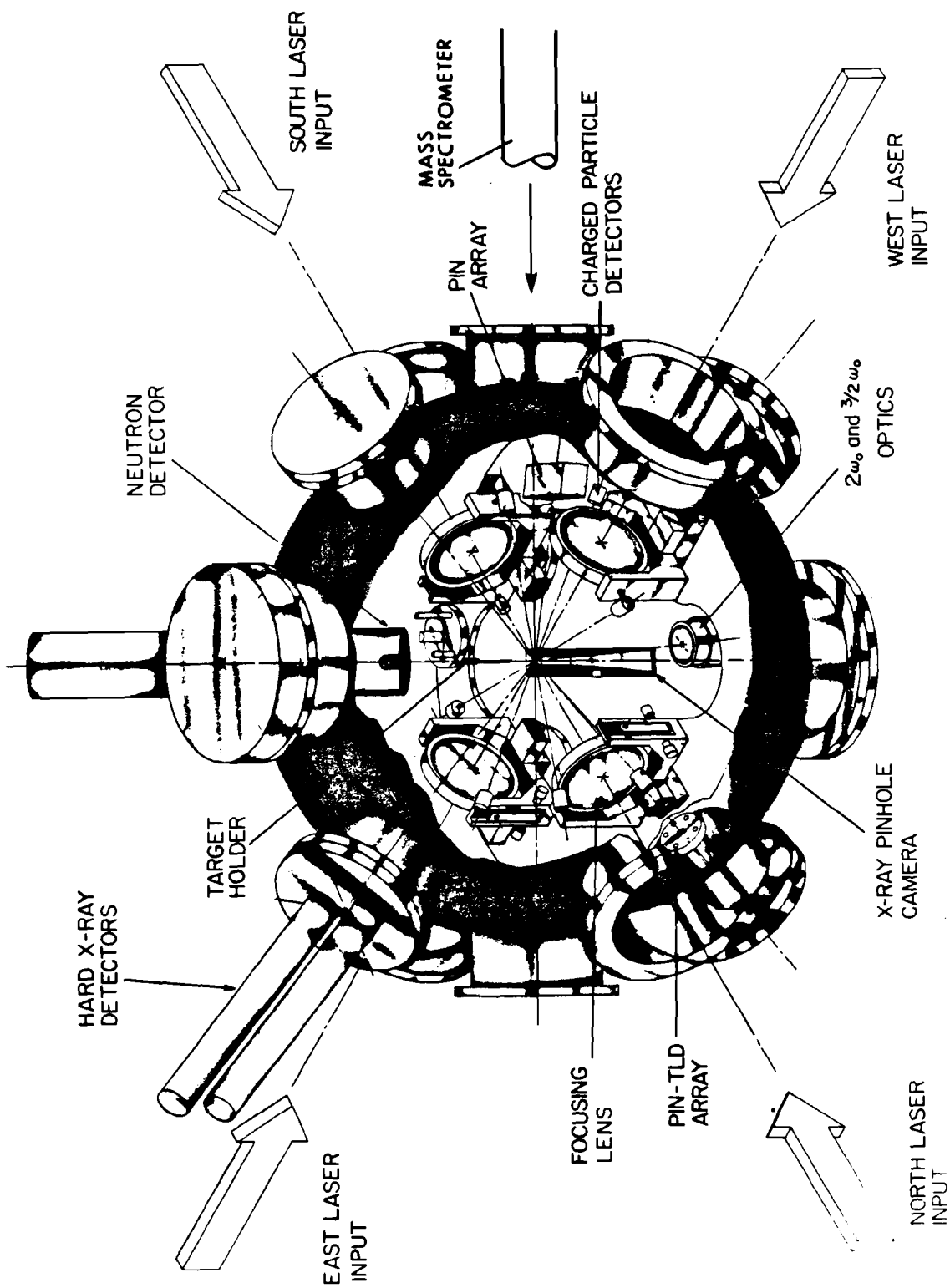

Figure 5. Configuration of the target irradiation facility.

target chamber and in particular there was one in the plane of illumination, a few degrees to each side of the port leading to the mass spectrometer. On each target shot, the charge collectors recorded the total ion current throughout the entire velocity range of the plasma. The mass spectrometer, on the other hand, could measure only a portion of this velocity range in a single shot due to instrumental limitations. This is best illustrated by examining the amount of information which the mass spectrometer obtains from a single target shot, such as shot 17685 which is shown in Figures 6 and 7. For convenience the oxygen and the silicon data for that shot have been plotted separately so that the various ionic species may be identified simply by using the ion's charge state.

As has been noted earlier, a single detector in the mass spectrometer measures a single ion energy per unit charge. This causes the detector to view a different velocity for each incident mass to charge ratio with the result that the instrument sees a much higher velocity range for the high charge states than it does for low charge states. This is emphasized in part B of the figures which shows that the data obtained for each charge state spans a different velocity range. In fact there is no velocity for which the instrument is capable of detecting all the possible ions in a single shot.

Most diagnostic devices for laser produced plasmas have great difficulty combining data obtained from separate target shots due to the irreproducibility of the laser pulse. Frequently the

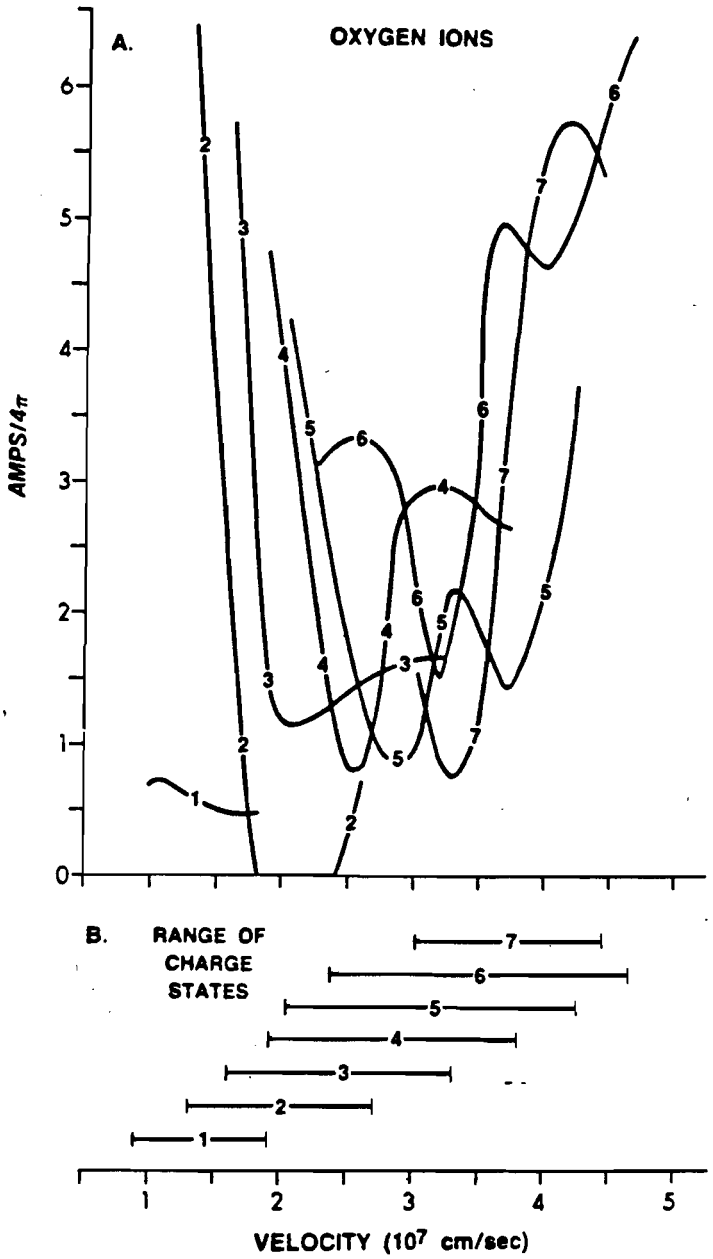

Figure 6.
Mass Spectrometer Data (Oxygen Ions, Shot 17685).

Part A. The ion current (±5%) for each of the oxygen charge states a function of velocity.

Part B. Emphasizes the velocity range over which the various charge states were detected.

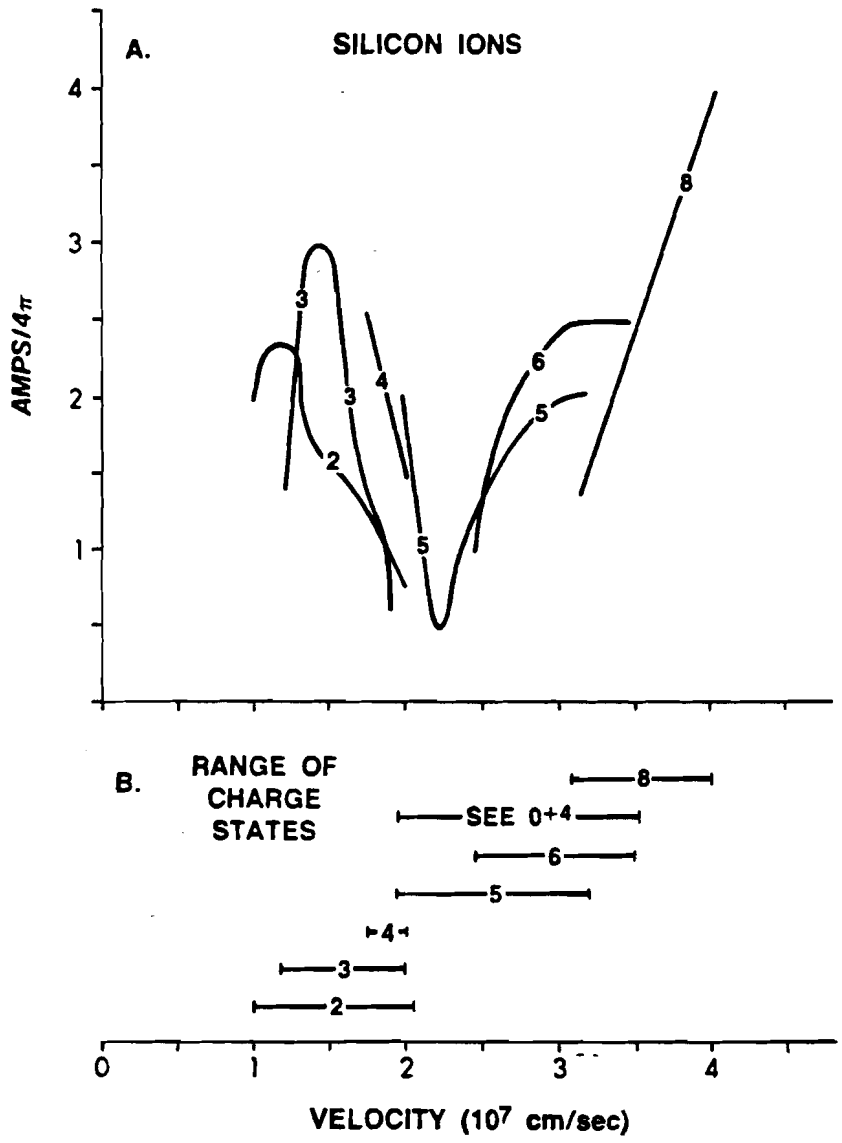

Figure 7.
Mass Spectrometer Data (Silicon Ions, Shot 17685).

Part A. The ion current (±5%) for each of the silicon charge states as a function of velocity.

Part B. Emphasizes the velocity range over which the various charge states were detected.

observed plasma parameter experiences large shot to shot fluctuations in response to subtle variations in the incident energy. However the average ion mass to charge ratio of the plasma (defined by equation 13) is not sensitive even to large changes in the incident energy.

$$\langle A/Z \rangle = \frac{\Sigma\ (A/Z)_\alpha\ I_\alpha}{\Sigma\ I_\alpha} \qquad (13)$$

where the index α denotes the different mass to charge ratios and their corresponding currents.

Experimental verification of this insensitivity is shown in Figure 8 where the measured mass to charge ratio for three different shots has been superimposed in the main portion of the figure. The insert in the upper right corner shows the total ion current for the three shots as measured by a charge collector:

	Shot #	Laser Energy	Target Diameter	Target Wall Thickness
1)	17685	8.4	64	0.67
2)	17687	6.4	69	0.66
3)	17672	1.7	60	0.76

All of these shots were viewed with the same voltage on the analyzing capacitor of the mass spectrometer so that the velocity examined for each ion mass to charge ratio was the same for all three shots. Despite the marked variation in the incident laser energy and the

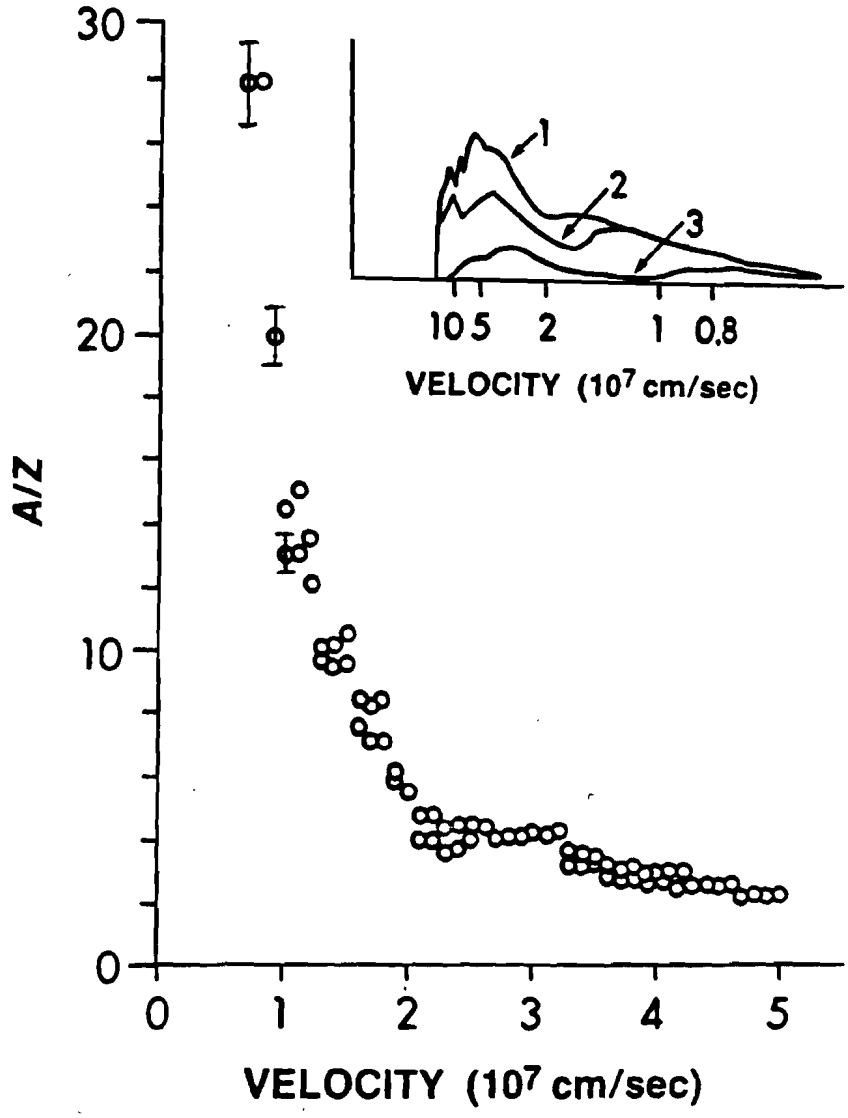

Figure 8.
The Independence of the Average Charge State from the Total Ion Current.

The inset shows the variation in the ion current due to differences in laser energy. Identical mass spectrometer settings were used to record the individual currents of the ion charge states for these same three shots: 1) 17685; 2) 17687; and 3) 17672. The corresponding average A/Z's are superimposed to show their similarity.

concomitant changes in the total ion current, the velocity dependence of the average mass to charge ratio did not change. The mass spectrometer did detect large fluctuations in the amplitude of the current carried by each type of ion, but when the current changed, it changed proportionately for all of the charge states present. Thus the average charge state did not change. As will be discussed in the next chapter, this independence of the charge distribution from parameters which affect the ion flux is an indication that recombination dominates the plasma late in the expansion after the ion flux has been determined.

Because the charge distribution does not change from shot to shot, it was possible to accumulate data from several similar shots and interpret it as if it were one shot. On different shots, different velocity ranges were examined by changing the voltage of the analyzing capacitor of the mass spectrometer. Sufficient data was taken so that sets of shots could be chosen to have similar target dimensions, incident energy, and ion current as measured by the charge collector cup closest to the mass spectrometer entrance. One such set consists of shots 17644, 17687, 17549, and 17561 for which the spectrometer voltage was set at 4000, 2000, 1000, and 500 volts respectively.

This choice of voltages changed the velocity window of the mass spectrometer in steps of $\sqrt{2}$, whereas on an individual shot the velocity range examined spanned a factor of 3. Thus there was a sub-

stantial overlap in the data obtained from different shots. By comparing the amplitude of the ion current for each charge state as measured by the mass spectrometer in the overlap region it was possible to guarantee that the parameters used to choose a set of shots were sufficient to select shots with the same ion current.

As an additional cross check on this process, the currents of all the individual ion species detected by the mass spectrometer were summed to simulate the total ion current that would enter a charge collector. This summed current should have the same general structure as is seen by the nearby charge collectors and it should account for the mass of the target. If an isolated mass spectrometer shot is subjected to this test it fails. The reason for this is evident in the example, shot 17685, of Figures 6 and 7. Because the current contributed by Oxygen 2 through 5 has not been accounted for at the slower velocities, and because the instrumental velocity cutoff varies with charge, two types of discrepancy appear. First the summed current is lower than that expected at the slower velocities. Second a series of jagged peaks appears in the summed current where the individual charge state measurements ended. Similar problems occur at the high velocity side of this shot (see Figure 9).

When a full set of shots is combined these problems disappear because the data becomes complete throughout the velocity range of interest. The average mass to charge ratio (see Figure 10) agrees

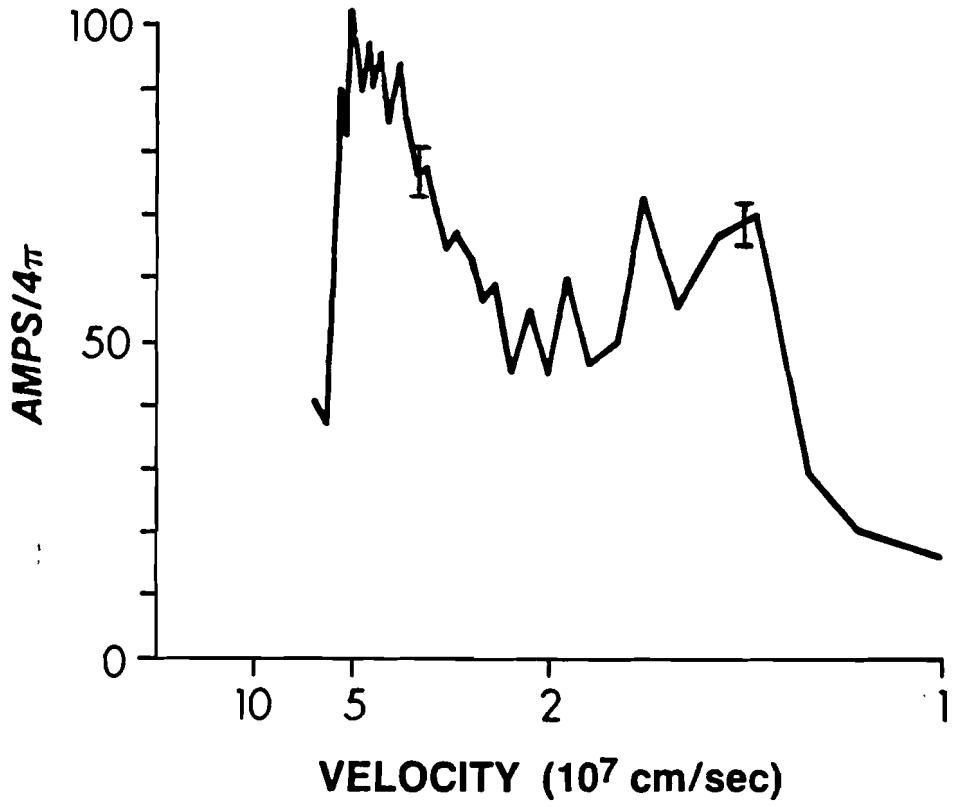

Figure 9.
Reconstruction of the Total Ion Current from a Single Mass Spectrometer Measurement.

The current shown is the result of summing the ion currents of the individual charge states measured. The absolute value shown assumes spherical symmetry at a distance of 25cm from the target.

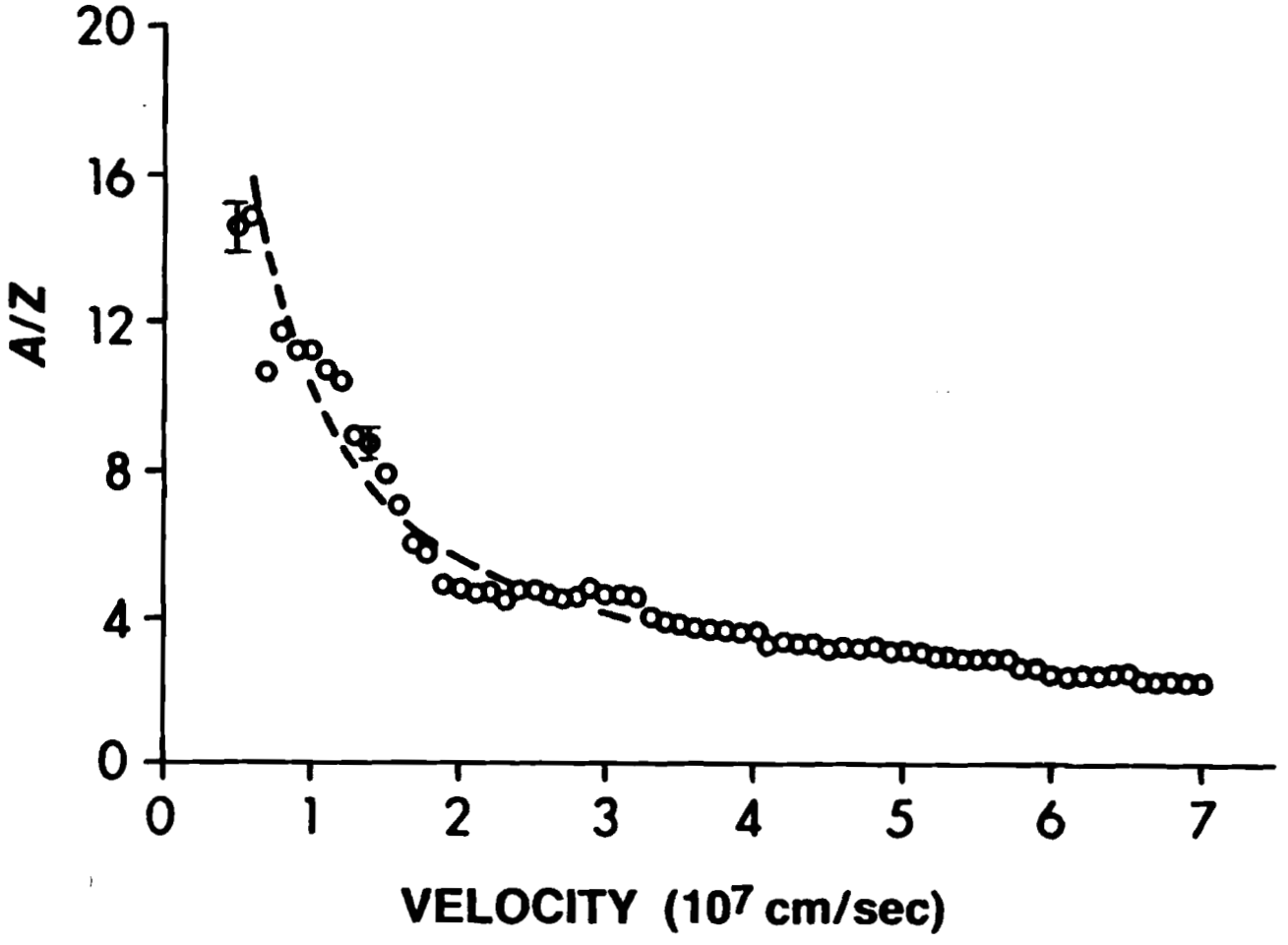

Figure 10.
Asymptotic Ion A/Z as a Function of Velocity

The measured average mass to charge ratio is indicated by dots. The analytic formula $9 \times 10^7 \, v^{-1} + 1.22$ (dashes) is shown as a convenient approximation to the measured values.

with that obtained by treating shots individually and averaging the results. The continuous range of the measured ion currents now spans the desired velocity interval. Using the results from the set of four shots mentioned above, summing the individual ion currents then yields a smooth curve. In Figure 11 this total ion current is compared to the current actually seen by a charge collector on one of the shots. The thermal peak (the faster of the two current peaks in the figure) is in quantitative agreement with the charge collector. The velocity of the slow peak is also in agreement. The quantitative discrepancy in the amplitude of the slow peak is not surprising. The charge collector is not expected to be quantitatively reliable for high currents at low velocity. Under these conditions it is possible for the charge density of the plasma within the charge collector to become high enough to grossly distort the bias potential which is used to strip the free electrons from the incident plasma. The charge collector saturates more easily at slow velocities because much more charge density is present for the same measured current.

The current that was seen by the charge collectors for the velocities of the slow peak is the expected saturation current[3] for the conditions of this experiment. The charge collectors were able to account for only 60% of the target mass while the higher current measured by the mass spectrometer is consistent with the mass of the entire target.

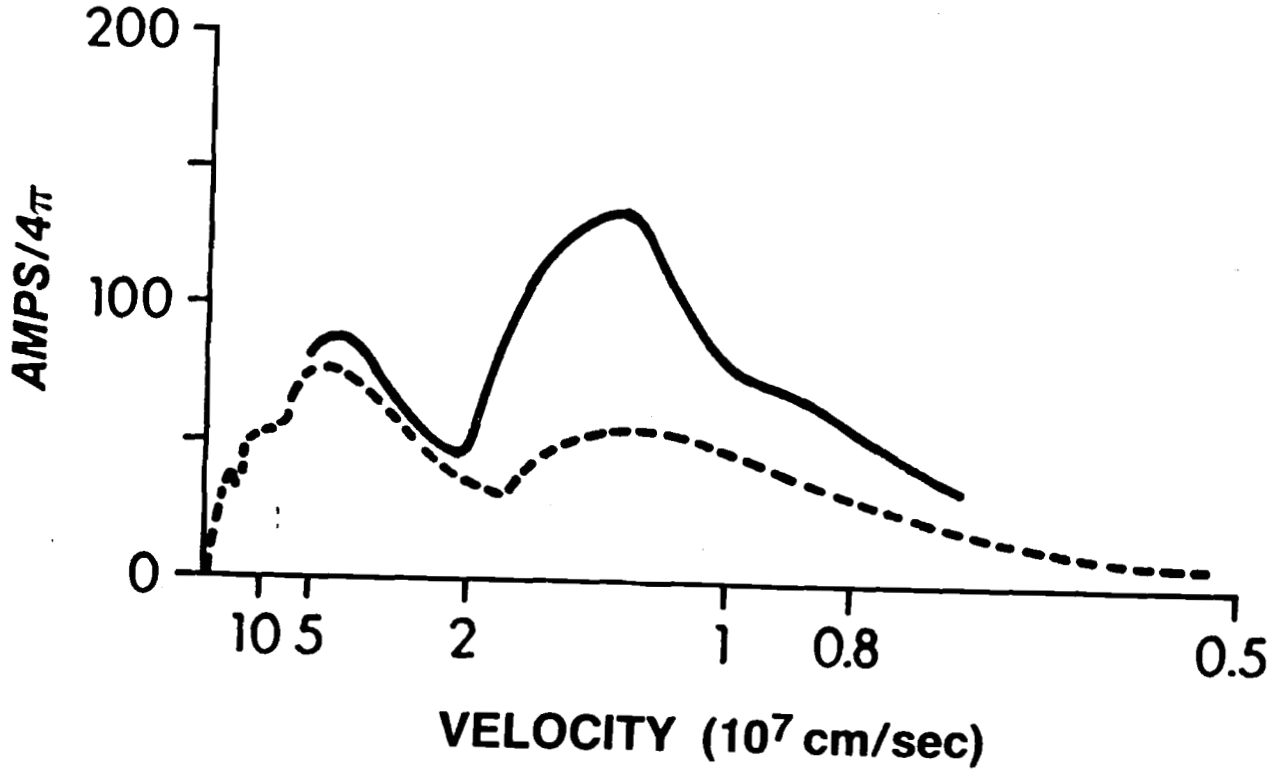

Figure 11.
Comparison of the Ion Currents Seen by the Mass Spectrometer and a Charge Collector.

The dashed line shows the charge collector current 25cm from the target for shot 17549. The mass spectrometer result (solid line) is derived by combining this shot and 3 similar shots. The abscissa assumes spherical symmetry.

REFERENCES - CHAPTER III

1. Slater, D. C. Private communication.

2. Pelah, I., Goldman, E. B. and Yaakobi, B. Phys. Rev. Lett. 37 829 (1976).

3. Green, T. S. Plasma Physics 12 877 (1970).

4. Yaakobi, B., Steel, D., et al. Phys. Rev. A 19 1247 (1979).

5. Thorsos, E., Delettrez, J., and Goldman, E. B. LLE 59 (August 1977).

CHAPTER IV

NUMERICAL SIMULATION OF THE ION CURRENT AND CHARGE STATE

It is well known that expanding plasmas created by short laser pulses have two distinct velocity components.[1,5,6,7] However previous measurements of the charge state distribution have been made only in the velocity region of the faster component.[1,8] Likewise previous numerical simulations[1,2,3,4] of the charge distribution have neglected the slower component of the plasma. This chapter will present the results of a simulation which includes both components of the expanding plasma and will compare those results to the measurements of the preceding chapter.

The calculations were done using the one dimensional hydrodynamic code LILAC. LILAC is a one-fluid, two-temperature, Lagrangian code. It includes energy transport via fast electrons, thermal conductivity (which is flux limited), and radiation. This allows the plasma dynamics to be calculated starting with the absorption of the laser energy.

Other simulations which have been compared to experiment[1,4] have used an expanding free streaming plasma to initialize their calculations. The initial density and velocity profiles were chosen by adiabatically scaling the measured asymptotic ion flux